

Global Flow of Glasma in High Energy Nuclear Collisions

Guangyao Chen, Rainer J. Fries

Cyclotron Institute and Department of Physics and Astronomy, Texas A&M University, College Station TX 77843, USA

Abstract

We discuss the energy flow of the classical gluon fields created in collisions of heavy nuclei at collider energies. We show how the Yang-Mills analogs of Faraday's Law and Gauss' Law predict the initial gluon flux tubes to expand or bend. The resulting transverse and longitudinal structure of the Poynting vector field has a rich phenomenology. Besides the well known radial and elliptic flow in transverse direction, classical quantum chromodynamics predicts a rapidity-odd transverse flow that tilts the fireball for non-central collisions, and it implies a characteristic flow pattern for collisions of non-symmetric systems $A + B$. The rapidity-odd transverse flow translates into a directed particle flow v_1 which has been observed at RHIC and LHC. The global flow fields in heavy ion collisions could be a powerful check for the validity of classical Yang-Mill dynamics in high energy collisions.

Keywords: Quantum Chromodynamics, Color Glass Condensate, Heavy Ion Collisions

PACS: 12.38.Mh, 24.85.+p, 25.75.-q

1. Introduction

Hadrons and nuclei colliding at very large energies can be used to study a novel regime of quantum chromodynamics (QCD) called the color glass condensate (CGC) [1]. It is characterized by a saturation of the transverse densities of gluons $\sim 1/Q_s^2$ in the initial wave functions, setting an energy scale Q_s , the saturation scale. High occupation numbers permit a quasi-classical description of the gluon fields in the nuclei before collisions [2, 3], and at very early time after the collision [4]. Data from the Relativistic Heavy Ion Collider (RHIC) and the Large Hadron Collider (LHC) have given us hints that we have reached an energy regime where CGC could be the correct description of the relevant degrees of freedom of early stages of nuclear collisions.

There is a large body of evidence that a thermalized quark gluon plasma (QGP) is eventually created within the first fm/c after the collision of nuclei at RHIC or LHC energies [5, 6]. CGC as an effective theory can be used to describe the very first step in this process, from the original nuclear wave functions to a space-time volume filled with

coherent and far off-equilibrium gluon fields, called a glasma, at a time $\tau_0 \sim 1/Q_s \sim 0.1 \dots 0.2$ fm/c after the collision. The dominant feature of the fields immediately after the collision are flux tubes of longitudinal chromo-electric and chromo-magnetic fields [7, 8, 9]. After this initial period the fields have to decohere and the emerging particles have to approach equilibrium [10, 11, 12]. After equilibrium is reached at a time $\tau_{th} > \tau_0$ hydrodynamics can be used to describe the global collective motion of the system [13, 14, 15, 16]. The success of hydrodynamics in heavy ion collisions is based on its ability to capture key features of the collective flow of the thermalized QGP, foremost the radial transverse flow v_r and the quadrupole asymmetry v_2 , called elliptic flow.

However, flow is not a privilege of thermalized matter with pressure gradients. In fact the effective "transverse pressure" $p_T = T^{11} = T^{22}$ in a purely longitudinal classical gauge field is equal to the energy density T^{00} , and thus gradients in pressure would be larger by a factor 3 than in a relativistic free gas with the same energy density [7, 17]. Thus the amount of initial collective motion, often termed pre-equilibrium flow, at the starting time τ_{th} of the hydrodynamic evolution is not ex-

Email address: rjfries@comp.tamu.edu
(Rainer J. Fries)

pected to be small. In fact various efforts have been made to estimate the magnitude of transverse flow around midrapidity from color glass or other dynamics [17, 18], although many hydrodynamics simulations still neglect pre-equilibrium flow.

In this Letter we expand existing calculations by analyzing the full 3+1-dimensional structure of the initial gluon energy flow. To that end we will present an analytic calculation of the chromo-electric and chromo-magnetic fields \vec{E} and \vec{B} immediately after the collision of nuclei in a strictly classical implementation of CGC, the McLerran-Venugopalan (MV) model [2, 3]. We then compute the energy momentum tensor $T^{\mu\nu}$ of the gluon field as a function of space-time coordinates for small proper times $\tau = \sqrt{t^2 - z^2}$ after the collision. We analyze the resulting global map of energy and momentum flow, in particular the transverse Poynting vector $S^i = T^{0i}$, $i = 1, 2$. We will argue that it can be decomposed into two parts, S_+^i and S_-^i . S_+^i is even in the space-time rapidity $\eta = 1/2 \ln[(t+z)/(t-z)]$ and driven by the gradient of the initial transverse pressure p_T of the gluon field; in short this term behaves “hydro-like” and has in fact been discussed before analytically and numerically [7, 17, 18]. The novel η -odd term S_-^i arises from asymmetries between the two nuclei, e.g. for collisions $A+B$ of different nuclei or for symmetric $A+A$ collision with finite impact parameter b . Since it vanishes at mid-rapidity it has not been discussed in situations where one expects flow to be (almost) boost-invariant. One can show that despite the superficial appearance the η -odd flow term S_-^i does not break the boost-invariance which is intrinsic to the MV model. We will argue, using the abelian case, that both rapidity-odd and -even terms are a natural consequence of Faraday’s Law and Gauss’ Law. We will conclude this Letter by discussing the phenomenological consequences for several colliding systems and impact parameters.

2. Gluon Fields in the MV Model

In the CGC the large momentum components of the nuclear wave function are assumed to be strongly Lorentz-contracted in the lab frame and can be approximated by an infinitely thin sheet. The large momentum quarks and gluons form an effective color $SU(3)$ charge density $\rho_a(\vec{r})$, $a = 1, \dots, N_c^2 - 1$, on that sheet, where \vec{r} is a transverse position. They act as sources for the soft gluon modes which are described by the classical field A^μ .

In the McLerran-Venugopalan model the source ρ_a moving along the $+$ -light cone leads to a $SU(3)$ -current $J^\mu = \delta^{\mu+} \delta(x^-) \rho_a t^a$ in light cone gauge. The soft gluon modes are determined by the Yang-Mills equation $D_\mu F^{\mu\nu} = J^\nu$. The charge density $\rho_a(\vec{r})$ varies on time scales that are large compared to typical time scales of the collision. It vanishes on average, $\langle \rho \rangle = 0$, due to local color neutrality, but has a non-vanishing variance μ which in the MV model is realized by a Gaussian distribution with

$$\langle \rho_a(\vec{r}_1) \rho_b(\vec{r}_2) \rangle = \frac{g^2}{N_c^2 - 1} \delta_{ab} \mu(\vec{r}_1) \delta^2(\vec{r}_1 - \vec{r}_2). \quad (1)$$

Thus μ is the average, *color-summed*, squared density of charges in the transverse plane (which differs from the definition in [19] by a factor $N_c^2 - 1$).

The most fundamental result of the MV model is an expression for the gluon distribution function of a nucleus in light cone gauge ($i, j = 1, 2$)

$$\langle A_a^i(\vec{r}) A_b^j(\vec{r}) \rangle = \frac{g^2}{8\pi(N_c^2 - 1)} \delta_{ab} \delta^{ij} \mu(\vec{r}) \ln \frac{Q^2}{m^2} \quad (2)$$

where the UV limit (both fields evaluated at the same transverse position \vec{r}) has been taken. Here Q is a UV cutoff related to the resolution with which the gluon distribution is probed and m is an infrared scale that can be introduced as an effective gluon mass. This result was first calculated in Ref. [20] for infinitely large, homogeneous nuclei, i.e. for constant source area density μ . Of course this is not a realistic approximation for nuclei. We have checked that if variations of $\mu(\vec{r})$ are permitted but are small on the IR length scale $\sim 1/m$, i.e.

$$m^{-1} |\nabla \mu(\vec{r})| \ll \mu(\vec{r}) \quad (3)$$

many well-known results of the MV model, in particular Eq. (2) hold and corrections can be classified in an expansion in gradients $m^{-1} \nabla^i \mu(\vec{r})$. In simple terms this indicates that the physics of color glass and the less known QCD dynamics at larger distances can be separated in a meaningful way as long as condition (3) is satisfied. We will report details of this calculation elsewhere [21].

Given the purely transverse gauge fields $A_1^i = A_{a,1}^i(\vec{r}) t^a$ and $A_2^i = A_{a,2}^i(\vec{r}) t^a$ of the nuclei before the collision, in their respective light cone gauge, one can write the longitudinal chromo-electric and -magnetic fields after the collision for small times τ

as [8, 21, 22]

$$E^3 = \left(1 + \frac{\tau^2}{4} D^2\right) E_0 + \mathcal{O}(\tau^4) \quad (4)$$

$$B^3 = \left(1 + \frac{\tau^2}{4} D^2\right) B_0 + \mathcal{O}(\tau^4) \quad (5)$$

where $D^2 = D^i D^i$ is the square of the covariant derivative with respect to gauge field $A_1^i + A_2^i$ and $E_0 = ig [A_1^j, A_2^j]$, $B_0 = ig \epsilon^{jk} [A_1^j, A_2^k]$ are the longitudinal fields at $\tau = 0$. Since the transverse fields vanish at $\tau = 0$ this has given rise to the notion of flux tubes of longitudinal electric and magnetic fields [9]. In terms of those initial longitudinal fields the transverse fields can be expressed as [8, 21, 22]

$$E^i = -\frac{\tau}{2} (\sinh \eta D^i E_0 + \cosh \eta \epsilon^{ij} D^j B_0) \quad (6)$$

$$B^i = -\frac{\tau}{2} (\sinh \eta D^i B_0 - \cosh \eta \epsilon^{ij} D^j E_0) \quad (7)$$

plus terms of order τ^3 and higher.

It is straightforward to write down the initial energy density $\epsilon_0 = T^{00}(\tau = 0) = (E_0^2 + B_0^2)/2$ and the initial transverse energy flux given by the Poynting vector T^{0i} . The leading behavior at small τ has four terms, two even in η ,

$$S_+^i = \frac{\tau}{2} \cosh \eta (E_0 D^i E_0 + B_0 D^i B_0), \quad (8)$$

and two odd in η ,

$$S_-^i = \frac{\tau}{2} \sinh \eta \epsilon^{ij} (E_0 D^j B_0 - B_0 D^j E_0), \quad (9)$$

and $T^{0i} = S_+^i + S_-^i$. The longitudinal energy flow is suppressed and starts at order $\mathcal{O}(\tau^2)$,

$$T^{03} = \frac{\tau^2}{8} [\sinh 2\eta ((DE_0)^2 + (DB_0)^2) + 2 \cosh 2\eta \epsilon^{ij} (D^i E_0)(D^j B_0)] \quad (10)$$

Note that the MV model is boost-invariant by definition and the η -dependence of the energy flow does not violate boost-invariance. One can verify that the full energy momentum tensor $T^{\mu\nu}$ satisfies $\Lambda^{\mu\mu'}(y) T_{\mu'\nu'}(\eta) \Lambda^{\nu\nu'}(y) = T_{\mu\nu}(\eta + y)$ where $\Lambda(y)$ is the Lorentz boost tensor with rapidity y along the z -axis. In fact the rapidity-odd field is a natural consequence of the field equations as the next section will show.

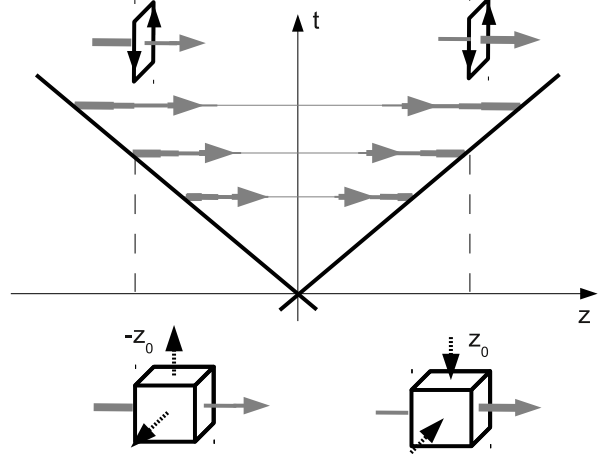


Figure 1: Two observers at $z = z_0$ and $z = -z_0$ test Ampère's and Faraday's Laws with areas a^2 in the transverse plane and Gauss' Law with a cube of volume a^3 . The transverse fields from Ampère's and Faraday's Laws (black solid arrows) are the same in both cases, while the transverse fields from Gauss' Law (black dashed arrows) are observed with opposite signs. Initial longitudinal fields are indicated by solid grey arrows, thickness reflects field strength.

3. An Electrodynamic Analogon

Let us consider the following equivalent boundary value problem in classical electrodynamics. In the forward light cone $\tau > 0$ we have the Maxwell Equations $\partial_\mu F^{\mu\nu} = 0$ without sources. On the light cone $\tau = 0$ we demand the boundary conditions $\vec{E}(\tau = 0, \vec{r}) = E_0(\vec{r})\vec{e}_z$, $\vec{B}(\tau = 0, \vec{r}) = B_0(\vec{r})\vec{e}_z$, i.e. the initial fields are purely longitudinal. We also assume that those fields are related through transverse fields A_1^i and A_2^i as $E_0 = \delta^{ij} A_1^i A_2^j$ and $B_0 = \epsilon^{ij} A_1^i A_2^j$. The abelian problem for fixed initial conditions can in principle be solved analytically [4, 21], but it will suffice here to give the solution order by order in powers of τ as we did in the case of QCD. From the QCD solutions we can immediately conclude that the longitudinal fields in the abelian case are

$$E^3 = \left(1 + \frac{t^2 - z^2}{4} \nabla^2\right) E_0 \quad (11)$$

$$B^3 = \left(1 + \frac{t^2 - z^2}{4} \nabla^2\right) B_0, \quad (12)$$

while the transverse fields are

$$E^i = \frac{z}{2} \nabla^i E_0 + \frac{t}{2} \epsilon^{ij} \nabla^j B_0 \quad (13)$$

$$B^i = \frac{z}{2} \nabla^i B_0 - \frac{t}{2} \epsilon^{ij} \nabla^j E_0, \quad (14)$$

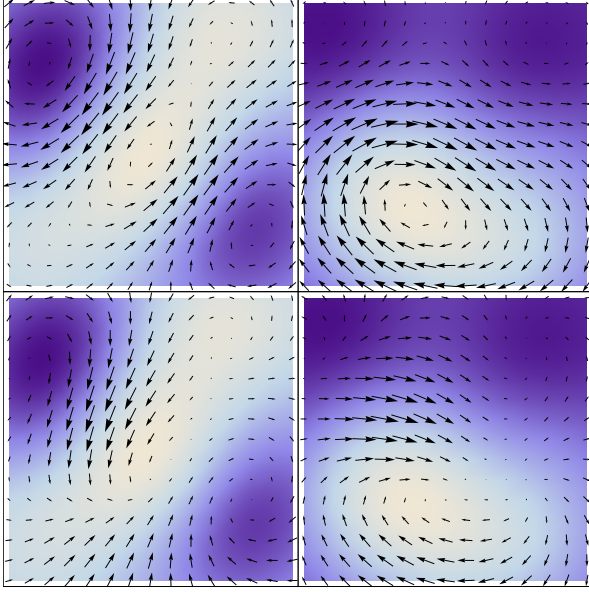


Figure 2: Transverse electric fields (left panels) and magnetic fields (right panels) at $\eta = 0$ (upper panels) and $\eta = 1$ (lower panels) in an abelian example for a random distribution of fields A_1^i, A_2^i . The initial longitudinal fields B_0 (left panels) and E_0 (right panels) are indicated through the density of the background (lighter color = larger values). At $\eta = 0$ the fields are divergence-free and clearly following Ampère's and Faraday's Laws, respectively.

for small times τ , i.e. $t^2 \approx z^2$. The cartesian coordinates permit simple checks of these solutions with Gauss', Ampère's and Faraday's Laws.

There is a straight-forward interpretation of some aspects of these results. Let us choose, just as an example, a transverse position where $E_0, B_0 > 0$ and $\nabla^2 E_0, \nabla^2 B_0 < 0$ so that the longitudinal fields decrease away from the light cone $t^2 = z^2$. Two observers at fixed points $z = z_0 > 0$ and $z = -z_0$ would observe the same electric (magnetic) flux through a small transverse area a^2 with an initial value $E_0 a^2$ ($B_0 a^2$) at $t = z_0$ which then diminishes at the same rate $\nabla^2 E_0 a^2 t/2$ ($\nabla^2 B_0 a^2 t/2$) for both. Due to Ampère's (Faraday's) Law this reduction induces magnetic (electric) fields curling with a negative (positive) chirality around the longitudinal fields, respectively, see Fig. 1.

On the other hand the same two observers at fixed points z_0 and $-z_0$ can at time $t = z_0$ count the electric or magnetic flux through small cubes of volume a^3 whose sides are aligned with the coordinate axes. One side is held at $z = \pm z_0$, while the opposite side is at $z = \pm z_0 \mp a$ for the observer at z_0 or $-z_0$ respectively. In the former case the total

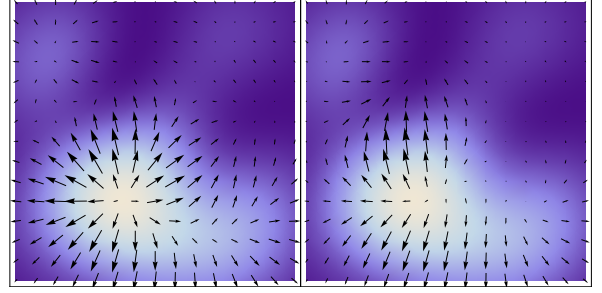


Figure 3: Example for transverse flow of energy for $\eta = 0$ (left panel) and $\eta = 1$ (right panel) in the abelian example for the same random distribution of fields A_1^i, A_2^i as in Fig. 2. The initial energy density T^{00} is shown through the density of the background (lighter color = larger values). At $\eta = 0$ the flow follows the gradient in the energy density in a hydro-like way while away from mid-rapidity energy flow gets quenched in some directions and amplified in others.

flux out of the box due to the longitudinal field is $-z_0 a^3 \nabla^2 E_0/2 > 0$ while for the observer at $-z_0$ the net flux of longitudinal field has the opposite sign. Thus at z_0 a net flux of transverse field has to enter into the box while at $-z_0$ the same amount has to flow out of the box to satisfy Gauss' Law.

To summarize, the transverse fields naturally have a part due to Gauss' Law with vanishing circulation ($\epsilon^{ij} \nabla^j$), which is odd in η , and they have a part due to Ampère's and Faraday's Law (and with different signs between the magnetic and electric part due to the Lenz rule) with vanishing transverse divergence (∇^i), which is even in η . Fig. 2 shows the transverse electric and magnetic fields for two rapidities η for random fields A_1^i and A_2^i in a sector of the transverse plane. One can check that this statement about transverse fields translates directly into a matching statement about the transverse flow of energy since the initial transverse Poynting vector is linear in the transverse fields, $T^{0i} = \epsilon^{ij} (E^j B_0 - B^j E_0)$. Thus we have the four contributions already discussed in the case of QCD, two of them odd in η . Fig. 3 shows the flux of energy in the transverse plane for two rapidities for the same random configuration of fields A_1^i, A_2^i .

4. Averaging Over Field Configurations

Eqs. (8), (9) can be the basis for a Monte Carlo modeling of the energy flow starting from a sampling of possible nuclear fields A_1^i, A_2^i or initial charge densities ρ_1^a, ρ_2^a in the colliding nuclei. Here we will present a calculation of the expectation

value of the flow fields carried out in the MV model with slowly varying average charge density μ . It has been shown in [19] that the expectation value of the initial energy density is given by the product of the average source densities μ_1, μ_2 in both nuclei,

$$\varepsilon_0(\vec{r}) = \frac{g^6}{32\pi^2} \frac{N_c}{N_c^2 - 1} \ln^2 \frac{Q^2}{m^2} \mu_1(\vec{r}) \mu_2(\vec{r}). \quad (15)$$

For the transverse Poynting vector let us discuss our expectations before calculating the result. First we note that the non-abelian terms from the covariant derivatives would lead to expectation values of three-gluon correlators $\langle AAA \rangle$ in one of the nuclei which under the assumptions of the McLerran-Venugopalan model vanish. Furthermore we can convince ourselves that because of the relation between E_0 and B_0 given by A_1^i and A_2^i the two terms in (9) are the same up to a sign and thus add up constructively. One can also easily argue that for dimensional reasons $\mu_1 \nabla^i \mu_2 + \mu_2 \nabla^i \mu_1$ and $\mu_1 \nabla^i \mu_2 - \mu_2 \nabla^i \mu_1$, and their contractions with ϵ^{ij} are the only four transverse vectors available after averaging.

The first option, symmetric in the two nuclei and circulation-free, is picked by the η -even flow term

$$\begin{aligned} S_+^i &= -\frac{\tau}{2} \cosh \eta \frac{g^6}{32\pi^2} \frac{N_c}{N_c^2 - 1} \ln^2 \frac{Q^2}{m^2} \nabla^i (\mu_1 \mu_2) \\ &= -\frac{\tau}{2} \cosh \eta \nabla^i \epsilon_0. \end{aligned} \quad (16)$$

It mimics hydrodynamic flow. For the η -odd flow term we need to know the expectation value of two gluon fields in light cone gauge with one derivative. Following the same recipe that leads to the expression (2) for the gluon distribution and using our smoothness condition on $\mu(\vec{r})$ we obtain

$$\begin{aligned} \left\langle \left(\partial^k A_a^i \right) (\vec{x}_\perp) A_b^j (\vec{x}_\perp) \right\rangle &= \frac{g^2}{16\pi(N_c^2 - 1)} \delta_{ab} \\ &\times \ln \frac{Q^2}{m^2} \nabla^l \mu(\vec{x}_\perp) (\delta^{jl} \delta^{ik} - \delta^{il} \delta^{jk} - \delta^{kl} \delta^{ij}) \end{aligned} \quad (17)$$

as the leading term contributing to S_-^i . We refer the reader to a detailed calculation of this correlation function in a forthcoming publication [21]. It is then straight forward to obtain the rapidity-odd flow as

$$\begin{aligned} S_-^i &= -\frac{\tau}{2} \sinh \eta \frac{g^6}{32\pi^2} \frac{N_c}{N_c^2 - 1} \\ &\times \ln^2 \frac{Q^2}{m^2} (\mu_2 \nabla^i \mu_1 - \mu_1 \nabla^i \mu_2). \end{aligned} \quad (18)$$

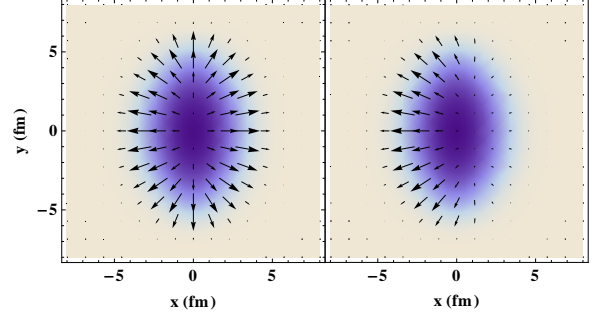


Figure 4: Flow field V^i (black arrows) and energy density ϵ_0 (shading) in the transverse plane for Au+Au collisions at $b = 6$ fm. The nucleus centered at $x = 3$ fm travels into the plane which is the positive η -direction. Left Panel: $\eta = 0$. Right Panel: $\eta = 1$.

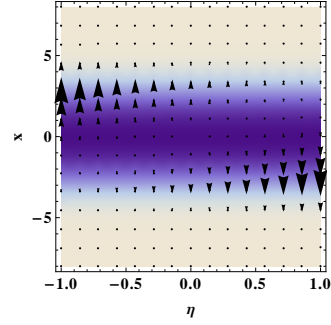


Figure 5: Same as Fig. 4 but plotted in the $\eta - x$ -plane defined by $y = 0$. The flow will lead to a tilted fireball.

5. Discussion of Results

To summarize, the prediction of classical QCD for the initial average transverse energy flow normalized by the average initial energy density is

$$\begin{aligned} V^i &= \frac{T^{0i}}{\epsilon_0} = -\frac{\tau}{2} \left(\cosh \eta \frac{\nabla^i (\mu_1 \mu_2)}{\mu_1 \mu_2} \right. \\ &\quad \left. + \sinh \eta \frac{\mu_2 \nabla^i \mu_1 - \mu_1 \nabla^i \mu_2}{\mu_1 \mu_2} \right) \end{aligned} \quad (19)$$

which is independent of the UV cutoff and the IR regulator. In the following we have calculated V^i in several situations using Woods-Saxon profiles for incident nuclei. Fig. 4 shows the average flow field V^i for the collision of two gold nuclei at impact parameter $b = 6$ fm in the transverse plane for two space-time rapidities. One can clearly see the evolution in rapidity from a hydro-like flow field at $\eta = 0$ to a preferred flow direction at forward rapidity.

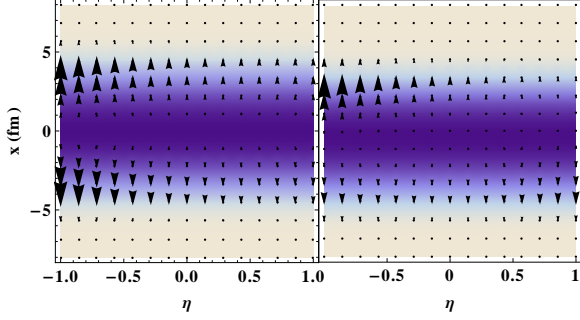


Figure 6: The same as Fig. 5 for Au+Cu (Au traveling to the right). Left Panel: $b = 0$ fm. Right Panel: $b = 2$ fm.

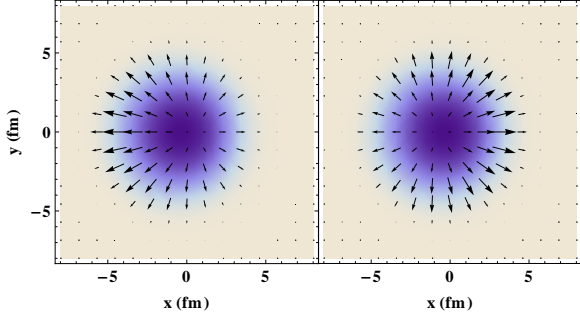


Figure 7: The same as Fig. 4 for Au+Cu at $b = 2$ fm. Left Panel: $\eta = 1$, Right Panel: $\eta = -1$.

In Fig. 5 the same collision is shown in the $\eta - x$ -plane. Clearly the flow tilts the fireball clockwise. The orientation of rotation is as if the gluon flux tubes preferred to expand in the wake of spectator nucleons in such a way that the flow increases with increasing separation from the spectators in rapidity. However this can not be taken literally as the origin of the effect. Our calculation is based on a small time expansion and the response of the energy density to the flow will come in at the next order. Note that the normalizations of the vector fields in the figures are arbitrary. Typical values of the flow V^i at the surface for Au+Au collisions is ~ 0.1 at $\tau = 0.1$ fm/c at midrapidity. Fig. 6 shows the average flow fields V^i for Au+Cu collisions at impact parameters $b = 0$ fm and $b = 2$ fm in the $\eta - x$ -plane. In the central case the flow field leads to an expansion which is much more pronounced on the Cu-side of the system, consistent with the rule of thumb that flux tubes like to expand into the wake of spectators (which here are solely from the gold nucleus). The flow pattern becomes more

involved for Au+Cu collisions at finite impact parameter. In Fig. 7 the flow in the transverse rapidity plane is shown for forward and backward rapidity for the $b = 2$ fm Au+Cu system. We notice that the azimuthal modulation of the flow is non-trivial but can again be understood through the position of spectator nucleons from the Au nucleus (centered at $x = 1$ fm). This and the previous figures make it clear that S_-^i contributes not only to directed flow but also to the elliptic flow.

The flow of energy in the classical field before τ_{th} will translate into a flow of energy in the hydrodynamic phase after thermalization due to local energy and momentum conservation [7]. One expects remnants of this flow to survive in hydrodynamics due to the inertia of fluid cells. In particular, this should result in a directed flow of particles which is odd in momentum rapidity y . In fact such a y -odd directed flow, measured by the first Fourier component v_1 , has been observed at RHIC [23, 24]. The sign of the effect is consistent with the expectation from color glass, moreover the data points as a function of rapidity could be fitted with a $\sinh y$ -shaped function. At this point it is too early to draw strong conclusions but the coincidence of sign and shape of the effect with data is encouraging.

Some of the qualitative features of the flow field discussed here have been generated in hydrodynamic simulations by initializing a tilted source [25], e.g. postulated in the fire streak model [26]. Our calculation suggests that color glass could account for this phenomenon without invoking additional model assumptions. In addition, classical QCD adds several unique predictions in particular for the case of collisions of asymmetric nuclei. A systematic study of flow as a function of rapidity and different nuclear systems could find this unique fingerprint of color glass.

RJF acknowledges many useful discussions with J. Kapusta and Y. Li and he is grateful for encouragement by L. McLerran. This project was supported by the U.S. National Science Foundation through CAREER grant PHY-0847538, and by the JET Collaboration and DOE grant DE-FG02-10ER41682.

References

- [1] F. Gelis, E. Iancu, J. Jalilian-Marian and R. Venugopalan, Ann. Rev. Nucl. Part. Sci. **60**, 463 (2010)
- [2] L. D. McLerran and R. Venugopalan, Phys. Rev. D **49**, 3352 (1994)

- [3] L. D. McLerran and R. Venugopalan, Phys. Rev. D **49**, 2233 (1994)
- [4] A. Kovner, L. D. McLerran and H. Weigert, Phys. Rev. D **52**, 3809 (1995); Phys. Rev. D **52**, 6231 (1995)
- [5] K. Adcox *et al.* [PHENIX Collaboration], Nucl. Phys. A **757**, 184 (2005)
- [6] J. Adams *et al.* [STAR Collaboration], Nucl. Phys. A **757**, 102 (2005)
- [7] R. J. Fries, J. I. Kapusta and Y. Li, Nucl. Phys. A **774**, 861 (2006)
- [8] R. J. Fries, J. I. Kapusta and Y. Li, preprint arXiv:nucl-th/0604054
- [9] T. Lappi and L. McLerran, Nucl. Phys. A **772**, 200 (2006)
- [10] R. J. Fries, B. Muller and A. Schafer, Phys. Rev. C **79**, 034904 (2009)
- [11] P. Romatschke and R. Venugopalan, Phys. Rev. D **74**, 045011 (2006) [hep-ph/0605045].
- [12] F. Gelis, S. Jeon and R. Venugopalan, Nucl. Phys. A **817**, 61 (2009) [arXiv:0706.3775 [hep-ph]].
- [13] P. F. Kolb and U. W. Heinz, in *Quark Gluon Plasma 3*, ed. R. C. Hwa et al., World Scientific (2003), preprint nucl-th/0305084
- [14] H. Song and U. W. Heinz, Phys. Rev. C **77**, 064901 (2008)
- [15] B. Schenke, S. Jeon and C. Gale, Phys. Rev. C **82**, 014903 (2010)
- [16] R. J. Fries and C. Nonaka, Prog. Part. Nucl. Phys. **66**, 607 (2011)
- [17] J. Vredevoogd and S. Pratt, Phys. Rev. C **79**, 044915 (2009)
- [18] B. Schenke, P. Tribedy and R. Venugopalan, Phys. Rev. Lett. **108**, 252301 (2012)
- [19] T. Lappi, Phys. Lett. B **643**, 11 (2006)
- [20] J. Jalilian-Marian, A. Kovner, L. D. McLerran and H. Weigert, Phys. Rev. D **55**, 5414 (1997)
- [21] G. Chen, R. J. Fries, J. I. Kapusta and Y. Li, in preparation
- [22] H. Fujii, K. Fukushima and Y. Hidaka, Phys. Rev. C **79**, 024909 (2009)
- [23] B. I. Abelev *et al.* [STAR Collaboration], Phys. Rev. Lett. **101**, 252301 (2008)
- [24] J. Adams *et al.* [STAR Collaboration], Phys. Rev. C **73**, 034903 (2006)
- [25] L. P. Csernai, V. K. Magas, H. Stocker and D. D. Strottman, Phys. Rev. C **84**, 024914 (2011)
- [26] J. Gosset, J. I. Kapusta and G. D. Westfall, Phys. Rev. C **18**, 844 (1978)